Generalized diagram technique and spin waves in an anisotropic ferromagnet

R. O. Zaĭtsev

I. V. Kurchatov Institute of Atomic Energy
(Submitted May 24, 1974)
Zh. Eksp. Teor. Fiz. **68**, 207–215 (January 1975)

A diagram technique is developed for finite-rank operators that commute at various sites of the crystal lattice. It is shown that the law of conservation of root vectors, which are a peculiar type of "latent" parameters of the problem, is satisfied at each vertex. Properties of an ideal ferromagnet of the easy plane type are studied in the low temperature limit. For frequencies lower than the anisotropy energy there is a logarithmic dispersion of the magnetic permeability tensor with components along the spontaneous-moment direction perpendicular to the crystal axis.

1. INTRODUCTION

We consider the simplest model of a ferromagnet, when the anisotropy has a single-ion character, and the exchange-interaction anisotropy can be neglected. In this case the Hamiltonian is

$$\mathcal{H}=\sum_{\mathbf{r}}[2D(\mathrm{nS}_{\mathbf{r}})^2-\mathrm{HS}_{\mathbf{r}}]-\frac{1}{2}{\sum_{\mathbf{rr}'}}' J(\mathbf{r}-\mathbf{r}')(\mathbf{S}_{\mathbf{r}}\mathbf{S}_{\mathbf{r}'}). \tag{1}$$

At finite temperatures and at $D>0$, this system was investigated by the self-consistent field method in[1,2]. At low temperatures, the spectrum was calculated in the spin-wave approximation[3]. Kashchenko-Balakhanov, and Kurbatov[4] have determined the fluctuation corrections to the spectrum, but in the limit as $T\to 0$ they make an exponentially small contribution. Westwanski[5] has developed a diagram technique for finding kinematic and dynamic corrections to the excitation spectrum and found them in second-order perturbation theory. Unfortunately, the sums over the momenta were not calculated, so that it is impossible to establish the temperature and frequency dependences of the obtained self-energy parts.

The present paper is devoted to a study of the singularities of the spin-wave spectrum and the magnetic permeability in the low-frequency limit. In the case $S=1$ and $D>0$, the spectrum has three branches, one of which is practically acoustic with a gap proportional to $\sqrt{DH}$. For frequencies of the order of the gap, production of a magnon pair is possible. The presence of a threshold leads to an anomalous behavior of the magnetic permeability in the frequency interval $T\ll\omega\ll D$, if $T\ll\sqrt{D}$.

2. DIAGRAM TECHNIQUE

If we separate the molecular field in the Hamiltonian (1), then we obtain at unity spin a system of three nonequidistant levels. It is shown in[6] that the interaction Hamiltonian can be expanded in a basis of eight operators of the SU(3) group. We set each off-diagonal operator in correspondence with a root vector $\boldsymbol{\alpha}$. The use of this concept turns out to be very convenient, inasmuch as the law of conservation of the summary root vector will be satisfied in each vertex[7].

The single-cell Hamiltonian can always be diagonalized, inasmuch as it can be represented, accurate to a constant, in the form of a linear combination of diagonal operators h with zero trace:

$$\mathcal{H}_1=-\sum_{rh}\lambda_h h_{hr}. \tag{2}$$

We assume that the operators h satisfy the orthogonality and normalization conditions

$$(h_k)_{ij}=s_k^i\delta_{ij},\quad \sum_k s_k^i s_k^i=\delta_{ij},\quad \mathrm{Sp}(h_k h_p)=\delta_{kp}. \tag{3}$$

The components of the root vectors are determined by the commutation relations (in one and the same cell)

$$[h_k, X^{pq}]=\alpha_k(p,q)X^{pq}. \tag{4}$$

The operator $X_{\mathbf{r}}^{pq}$ has a single unique matrix element at the intersection of the p-th row and q-th column, so that

$$\alpha_k(p,q)=s_k^p-s_k^q.$$

Direct calculation shows that the commutator of two conjugate operators takes the form

$$[X^{pq}, X^{qp}]=\sum_k \alpha_k(p,q)h_k. \tag{5}$$

A commutator of two non-conjugate operators is written in the form

$$[X_\alpha, X_\beta]=N_{\alpha,\beta}X_{\alpha+\beta}\quad (X_\alpha\equiv X_{\alpha(p,q)}\equiv X^{pq}). \tag{6}$$

Using the Jacobi identity, we can show[8,9] that the coefficient $N_{\alpha\beta}$ vanishes if $\alpha+\beta$ is not a root vector. In all the remaining cases $N_{\alpha,\beta}=\pm 1$. For an anticommutator there is satisfied the analogous relation

$$\{X_\alpha, X_\beta\}=N_{\alpha,\beta}^{(+)}X_{\alpha+\beta}, \tag{6'}$$

which can be obtained from the generalized Jacobi identity

$$[h_k\{X_\alpha X_\beta\}]=\{X_\alpha[h_k X_\beta]\}+\{X_\beta[h_k X_\alpha]\}.$$

We write down the operators of a multicell Hamiltonian in the form of a linear combination of diagonal operators h and off-diagonal operators in the interaction representation

$$X_\alpha(\tau)=e^{\tau\mathcal{H}_1}X_\alpha e^{-\tau\mathcal{H}_1}=X_\alpha e^{-\tau(\lambda\alpha)}.$$

The most general form of a two-cell Hamiltonian is the following:

$$\mathcal{H}_2=-\frac{1}{2}{\sum_{\mathbf{rr}'\alpha\beta}}' V_{\alpha,\beta}(\mathbf{r}-\mathbf{r}')X_{\alpha\mathbf{r}}X_{\beta\mathbf{r}'}-{\sum_{\mathbf{rr}'\alpha h}}' V_{h\alpha}(\mathbf{r}-\mathbf{r}')\Delta h_{h\mathbf{r}}X_{\alpha\mathbf{r}'} \tag{7}$$
$$-\frac{1}{2}{\sum_{\mathbf{rr}'hp}}' V_{hp}(\mathbf{r}-\mathbf{r}')\Delta h_{h\mathbf{r}}\Delta h_{p\mathbf{r}'};$$
$$\Delta h_{k\mathbf{r}}=h_{k\mathbf{r}}-\langle h_k\rangle$$

The interaction $V_{\mathbf{a},\mathbf{b}}(\mathbf{r}-\mathbf{r}')$ will be represented in the form of a wavy line with the indices $\mathbf{ar}$ and $\mathbf{br}'$ on the ends. If the index corresponds to the root vector $\boldsymbol{\alpha}$, then an outward arrow is placed on the corresponding end (see Fig. 1).

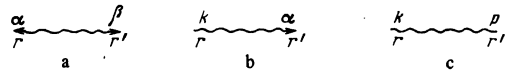

FIG. 1. Different types of interaction: a–$V_{\alpha\beta}(r-r')$, b–$V_{k\alpha}(r-r')$, c–$V_{kp}(r-r')$.

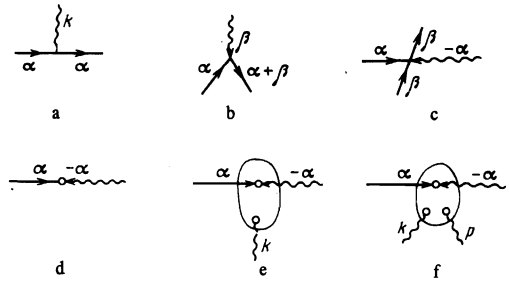

FIG. 2. Different types of vertices.

The construction of the diagram technique is based on the generalized Wick theory, which was established for spin operators in the paper of Vaks, Larkin, and Pikin[10]:

$$\langle T(u_{a_1}(\tau_1)u_{a_2}(\tau_2)\dots u_{a_{k-1}}(\tau_{k-1})X_\alpha(\tau)u_{a_k}(\tau_k)\dots u_{a_p}(\tau_p))\rangle_0 \tag{8}$$
$$=\sum_{s=1}^{p} G_\alpha(\tau-\tau_s)\langle T(u_{a_1}(\tau_1)\dots u_{a_{s-1}}(\tau_{s-1})[X_\alpha u_{a_s}]_\tau u_{a_{s+1}}(\tau_{s+1})\dots u_{a_p}(\tau_p))\rangle_0,$$

$$G_\alpha(\tau)=e^{-\tau(\lambda,\alpha)}\left\{\begin{matrix}1+N(\lambda\alpha) & \text{for } \tau>0\\ N(\lambda\alpha) & \text{for } \tau<0\end{matrix}\right\}=T\sum_{\omega_n}\frac{e^{-i\omega_n\tau}}{-i\omega_n+\alpha\lambda}. \tag{9}$$

Following[10], we represent the function $G_\alpha(\tau-\tau')$ in the form of a solid line with a vector index α, leaving τ and entering τ'.

It is easily seen that each commutation relation corresponds to its own type of vertex. Thus, commutator (4) yields a vertex without a change in the root vector but with a factor $-\alpha_k$ (see Fig. 2a). The presence of relations (5) and (6) leads to vertices where the total root vector is conserved. The vertex in Fig. 2b has a factor $N_{\alpha,\beta}$. Figure 2c shows a vertex corresponding to relations (5) and (4). It should be preceded by the factor $-(\boldsymbol{\alpha}\cdot\boldsymbol{\beta})$.

The remaining vertices are analogous to those that arise in the spin technique (Figs. 2d, e, f, etc.). The circle in which the α-line terminates represents the factor

$$b(\alpha)=\sum_k \alpha_k\langle h_k\rangle_0=T\sum_k\alpha_k\frac{\partial(\ln Z)}{\partial\lambda_k},$$
$$Z=\mathrm{Sp}\left(\exp\frac{1}{T}\sum_s\lambda_s h_s\right). \tag{10}$$

The blocks enclosed in the oval line are determined by the derivative of the zeroth-approximation partition function (Z)

$$\Gamma^{(p)}_{k_1k_2\dots k_p}=T^p\partial^p(\ln Z)/\partial\lambda_{k_1}\partial\lambda_{k_2}\dots\partial\lambda_{k_p} \tag{11}$$

The operator X_α must be commuted not only with the operators of the interaction Hamiltonian. For each of the five presented possibilities, there is a situation in which the corresponding operator is an end operator, i.e., no wavy line reaches it. This circumstance can be taken into account by representing the same vertices, but with the interaction line crossed out. It is convenient to draw instead of a crossed-out interaction line an outgoing solid line but with the opposite root vector (see Fig. 3).

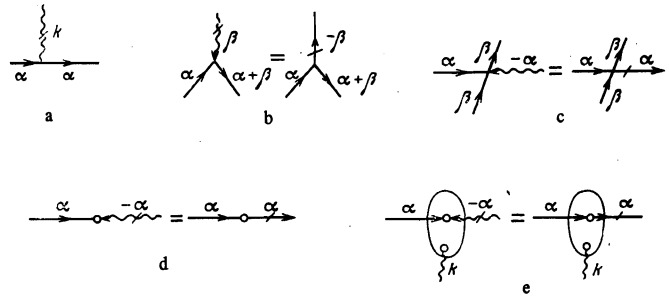

FIG. 3. Different types of end diagrams.

A detailed exposition of the generalized diagram technique can be found in the author's papers[7,11].

3. FERROMAGNET OF THE EASY PLANE TYPE

Assume that the external field is directed along the z axis, and the crystal axis coincides with the x axis. The Hamiltonian (1) can be rewritten in the form

$$\mathcal{H}_1=\sum_r(2D(S_r^z)^2-\bar{H}S_r^z);$$
$$\mathcal{H}_2=-\frac{1}{2}{\sum_{rr'}}' J(\mathbf{r}-\mathbf{r}')\Delta S_r^z\Delta S_{r'}^z-\frac{1}{2}{\sum_{rr'}}' J(\mathbf{r}-\mathbf{r}')S_r^+S_{r'}^-; \tag{12}$$

Here $\bar{H}=H+J(0)\langle S^z\rangle$ is the molecular field

$$\Delta S_r^z=S_r^z-\langle S^z\rangle,\quad S_r^\pm=S_r^x\pm iS_r^y.$$

For unity spin, it is easy to find the eigenvalues and the eigenfunctions of the single-cell Hamiltonian

$$\varepsilon_{1,3}=D\mp(D^2+\bar{H}^2)^{1/2},\quad \varepsilon_2=-2D,$$
$$\psi_1=\begin{pmatrix}\cos\theta\\0\\\sin\theta\end{pmatrix},\quad \psi_2=\begin{pmatrix}0\\1\\0\end{pmatrix},\quad \psi_3=\begin{pmatrix}-\sin\theta\\0\\\cos\theta\end{pmatrix};$$
$$\cos 2\theta=\frac{\bar{H}}{(\bar{H}^2+D^2)^{1/2}},\quad \sin 2\theta=-\frac{D}{(\bar{H}^2+D^2)^{1/2}}.$$

In the new representation, the single-cell Hamiltonian is diagonal. It can be reduced to the form (2) by using two diagonal operators

$$h_1=\frac{1}{\sqrt{2}}\begin{pmatrix}1&0&0\\0&0&0\\0&0&-1\end{pmatrix}\quad h_2=\frac{1}{\sqrt{6}}\begin{pmatrix}1&0&0\\0&-2&0\\0&0&1\end{pmatrix},$$

which satisfy the conditions (3). In this case

$$\lambda=\{[2(\bar{H}^2+D^2)]^{1/2},\ \sqrt{2/3}D\}.$$

Using (4), we obtain the well-known root system of the SU(3) group–see Fig. 4, with

$$\alpha(1.3)=(\sqrt{2}.0),\quad \alpha(1.2)=\left(\frac{1}{\sqrt{2}},\sqrt{\frac{3}{2}}\right),$$
$$\alpha(2.3)=\left(\frac{1}{\sqrt{2}},-\sqrt{\frac{3}{2}}\right),\quad \alpha(p,q)=-\alpha(q,p).$$

The numbers 1, 2, 3 in the arguments label the rows and the columns.

We express the spin operators in terms of the para-

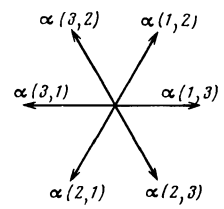

FIG. 4. Root system.

meter θ, and then expand them in the operators h_k and X_α:

$$S_r^+=(S_r^-)^+=\sqrt{2}\{\cos\theta(X_r^{12}+X_r^{23})+\sin\theta(X_r^{21}-X_r^{23})\},$$
$$S_r^z=\sqrt{2}\cos 2\theta h_{1r}-\sin 2\theta(X_r^{13}+X_r^{31}). \quad (13)$$

The interaction Hamiltonian takes the form (7). The matrix $\hat{V}(k)-J(k)$ is the direct product of two matrices:

$$\begin{array}{c} \\ \alpha(1,2) \\ \alpha(2,1) \\ \alpha(2,3) \\ \alpha(3,2) \end{array} \begin{array}{c} \begin{array}{cccc} \beta(1,2) & \beta(2,1) & \beta(2,3) & \beta(3,2) \end{array} \\ \begin{pmatrix} \sin 2\theta & 1 & 0 & \cos 2\theta \\ 1 & \sin 2\theta & \cos 2\theta & 0 \\ 0 & \cos 2\theta & -\sin 2\theta & 1 \\ \cos 2\theta & 0 & 1 & -\sin 2\theta \end{pmatrix} \end{array},$$

$$\begin{array}{c} \\ \alpha(1,3) \\ \alpha(3,1) \end{array} \begin{array}{c} \begin{array}{cc} \beta(1,3) & \beta(3,1) \end{array} \\ \begin{pmatrix} \sin^2 2\theta & \sin^2 2\theta \\ \sin^2 2\theta & \sin^2 2\theta \end{pmatrix} \end{array}.$$

At low temperatures in the "spin wave" approximation, and also in the self-consistent-field approximation (for long-range potentials), we obtain as the zero-order approximation the following system of equations for Green's function

$$[D_{\alpha,\beta}(k,\omega_n)]^{-1}\approx[D^{(0)}_{\alpha,\beta}(\omega_n)]^{-1}-V_{-\alpha,\beta}(k). \quad (14)$$

Here $D^{(0)}_{\alpha,\beta}(\omega_n)=\delta(\alpha-\beta)G_\alpha(\omega_n)b(\alpha)$, $\omega_n=2\pi nT\neq 0$,

$$D_{\alpha,\beta}(k,\omega_n)=\sum_r\int_0^{1/T}\exp(i\omega_n\tau-ikr)\langle T(\hat{X}_{\alpha r}(\tau)\hat{X}_{-\beta 0}(0))\rangle_0 d\tau.$$

The functions $G_\alpha(\omega_n)$ and $b(\alpha)$ are defined in (8) and (10). The longitudinal correlation function $\langle T(\Delta\hat{S}^z(x)\Delta\hat{S}^z(0)\rangle$ has poles under the condition $\det[D^{-1}_{\alpha,\beta}(k,i\omega_n\to\omega+i\delta)]=0$, $\alpha,\beta=\pm\alpha(1,3)$. With the aid of (14) we obtain

$$\omega_\parallel^2=(\lambda\alpha(1,3))^2-2b(1,3)\sin^2 2\theta J(k)(\lambda\alpha(1,3)).$$

At T = 0, b(1,3) = 1 and $\lambda\alpha(1,3)=2(\bar{H}^2+D^2)^{1/2}$ we have

$$\cos 2\theta=\frac{\bar{H}}{(\bar{H}^2+D^2)^{1/2}}=\frac{\bar{H}-H}{J(0)},$$

so that

$$\omega_\parallel^2=4\left(\bar{H}^2+D^2-\frac{D^2J(k)}{(\bar{H}^2+D^2)^{1/2}}\right). \quad (15)$$

The transverse correlation function has two pairs of symmetrically disposed poles. At T = 0, when b(1, 3) = b(1, 2) = 1 and b(2, 3) = 0, we have

$$\omega_\perp^2=[(\bar{H}^2+D^2)^{1/2}+D-J(k)]^2-(J(k)D)^2/(\bar{H}^2+D^2),$$
$$\omega=\pm(-D+(\bar{H}^2+D^2)^{1/2}).$$

We note that at H = 0 we have

$$\omega_\perp^2=[J(0)-J(k)]\left(1+\frac{D}{J(0)}\right)\left[J(0)-J(k)+D\left(1+\frac{J(k)}{J(0)}\right)\right], \quad (16)$$

so that as $k\to 0$ we have $\omega_\perp\sim ck$, where

$$c^2=-2J'(0)D[1+D/J(0)]. \quad (17)$$

On the other hand, if k = 0 and $H\ll D$, then

$$\omega_\perp\approx(2DH)^{1/2}\left(\frac{J(0)+D}{J(0)-D}\right)^{1/4}. \quad (18)$$

The longitudinal branch is optical. As $H\to 0$ and $k\to 0$ we have

$$\omega_\parallel^2=4(J^2(0)-D^2),$$

so that the system becomes unstable at anomalously large anisotropy (D > J(0)).

Let us consider a real situation when $D\ll J(0)$. It is easily seen that in the limit of the lowest temperature $T\ll D$, the expansion of the exact Green's function is in powers of $[D/J(0)]^{1/2}$, but in the limit of small frequencies and momenta the smallness of the "interaction constant" $[D/J(0)]^{1/2}$ may be offset by the large value of the logarithm

$$L=\ln(D^2/\lambda),\quad \lambda=\max\{\omega^2,\ 2DH,\ (ck)^2\}. \quad (19)$$

To separate the logarithmic diagrams, we consider the simplest corrections to the Green's function, which are shown in Figs. 5 and 6.

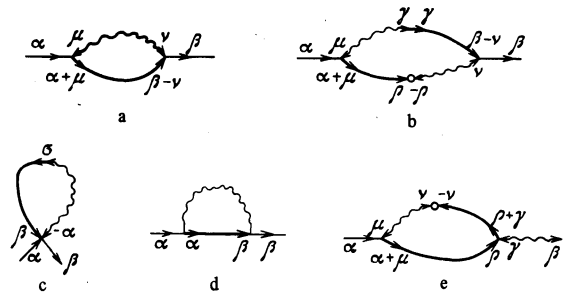

FIG. 5. Simplest self-energy parts.

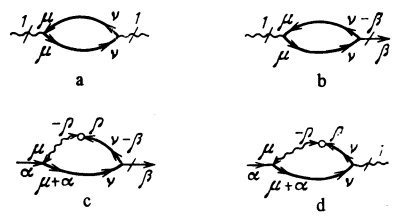

FIG. 6. Singular end diagrams.

The thick lines represent the G functions in the zeroth approximation ($\omega_n\neq 0$)

$$[G_{\alpha,\beta}(k,\omega_n)]^{-1}=[G^0_{\alpha,\beta}(\omega_n)]^{-1}-b(\alpha)V_{-\alpha,\beta}(k). \quad (20)$$

The thick wavy lines represent the effective interaction line $\Gamma_{\alpha,\beta}(k,\omega_n)$, calculated with the aid of the equations

$$\Gamma_{\alpha,\beta}(k,\omega_n)=V_{\alpha,\beta}(k)+\sum_{\alpha'}V_{\alpha,\alpha'}(k)G_{\alpha'}(\omega_n)b(\alpha')\Gamma_{-\alpha',\beta}(k,\omega_n). \quad (21)$$

From a comparison of (20) and (14) it follows that in the zeroth approximation the G function differs from the D function by the factor

$$D_{\alpha,\beta}=b(\beta)G_{\alpha,\beta}.$$

Figure 5 shows the usual self-energy parts, whereas Fig. 6 shows the simplest end diagrams.

If the temperature equals zero, and the level with number 1 is the lowest (D < J(0)), then the Green's function for the transitions $1\rightleftarrows 2$ is conveniently written in terms of Pauli matrices (see Eq. (20)):

$$G^{-1}=-i\omega_n+\tau a(k),$$
$$a_x=0,\quad a_y=-i\sin 2\theta J(k),\quad a_z=D-J(k)+(\bar{H}^2+D^2)^{1/2}. \quad (22)$$

(in the limit as $H\to 0$ we have $a_z\to D+J(0)-J(k)$). The first row (column) corresponds to the root vector $\alpha(1,2)$, and the second row (column) corresponds to the opposite vector. With the aid of (10) we can find the remaining Green's functions, but their explicit form will not be needed. The point is that the logarithmic integrals appear only in the case when the diagram contains not less than two Green's functions (22). The remaining functions do not contain singularities in the limit of

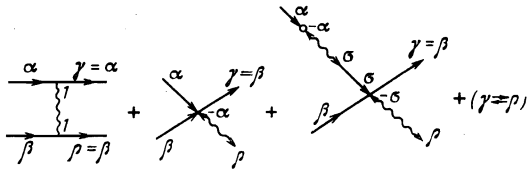

FIG. 7. Spin-wave scattering.

small **k** and therefore do not give rise to logarithmic integrals.

Using the conservation law, we can establish that in the lowest approximation a logarithmic behavior is exhibited by diagrams having on the ends the root vectors $\pm\alpha(1, 3)$. Each of these self-energy diagrams (see Fig. 5a, b, and e) yields a correction of order $[j(0)D]^{1/2}L$ to the $1 \rightleftarrows 3$ transition frequency. However, the main contribution of all these diagrams is cancelled, so that as a result we have a relative correction of order $[D/J(0)]^3L$.

The end diagrams shown in Fig. 6 do not cancel out. As seen from (13), the largest contribution to the longitudinal correlation function $\langle T(\Delta S_r^z(t)\Delta S_{r'}^z(t'))\rangle$ is made by the end diagram coming from the two operators h_1 (Fig. 6a). The singular diagrams shown in Figs. 6b, d, c enter respectively with a factor $\sin 2\theta$ and $\sin^2 2\theta$, and are not taken into account below.

The scattering of acoustic excitations by one another is determined by three types of vertices which are irreducible with respect to the transitions $1 \rightleftarrows 2$ (see Fig. 7). The vectors α, β, γ and ρ are acoustic, i.e., they correspond to $1 \rightleftarrows 2$ transitions, whereas the vector σ is optical (otherwise the third diagram would have to be attributed to the second). Each of the vertices of order J(0), but at $k = \omega = 0$ and $D = \theta = 0$ there is complete cancellation. For this reason, the logarithmic corrections due to the vertices contain an extra factor D/J and can become significant under the condition $(D/J)^{3/2}L \sim 1$. On the other hand, if the logarithm is not too large $(D/J)^{3/2}L \ll (D/J)^{1/2}L \lesssim 1$, then it suffices to take into account the simplest contribution of the diagram shown in Fig. 6a.

In the limit $T \ll \max(|\omega|, \sqrt{DH}, ck)$ we have

$$K_{zz}(\omega, k) = \frac{D^2}{4\pi^2 c^3} \ln\left[\frac{D^2}{\max[\omega^2, DH, (ck)^2]}\right]. \qquad (23)$$

CONCLUSION

Thus, the magnetic permeability has an anomalous dispersion in the frequency interval $\sqrt{DH} < \omega < D$, where it increases logarithmically with decreasing frequency. In the presence of a field in the region of the lowest frequencies $T \ll \omega \ll \sqrt{DH}$, the permeability is constant but is larger by a factor $\sqrt{D/J}\ln(D/H)$ than its value at $\omega \sim D$. If $H = 0$, then for sufficiently low frequencies $\omega < \mathrm{Dexp}(-\sqrt{J/D})$ formula (23) may turn out to be inaccurate, whereas at $\omega < \mathrm{Dexp}[-J/D)^{3/2}]$ it is certainly incorrect. It can be assumed that it is precisely in this region that the growth of the susceptibility should cease.

For frequencies $\omega > \sqrt{8DH}$, the longitudinal permeability acquires an imaginary part which is connected with the possibility of production of two magnons. The imaginary part, calculated in second-order perturbation theory (see Figs. 5 and 6) does not contain a large logarithm. For this reason, it is impossible to trace the frequency dependence of the surface impedance for $\omega \sim \sqrt{8DH}$. It can only be stated that there is no absorption at $\omega \ll \sqrt{DH}$. In the frequency region $D > \omega \gg \sqrt{DH}$, the imaginary part can be easily calculated by perturbation theory. The final result is simple: it is necessary to add to L the quantity $i\pi\theta$ $(\omega^2 - 8DH)$. Thus, at $H = 0$ the dispersion near the threshold takes the form $\ln(D^2/\omega^2) + i\pi$, and has nothing in common with the usual dispersion curve (of the Debye or of the Lorentz type). It can be shown that in a real situation this dependence vanishes when the frequency becomes smaller than the reciprocal spin-relaxation time or lower than the temperature. For this reason, one can attempt to observe the logarithmic anomaly at sufficiently low temperatures in anisotropic ferrodielectrics that are close to ideal.

The author is sincerely grateful to Prof. I. E. Dzyaloshinskiĭ for useful remarks and for interest in the work.

[1]V. N. Kitaev, M. P. Kashchenko, and L. V. Kurbatov, Zh. Eksp. Teor. Fiz. **65**, 2334 (1973) [Sov. Phys.-JETP **38**, 1166 (1973)].
[2]V. N. Kitaev, M. P. Kashchenko, L. V. Kurbatov, V. N. Kut'ko, V. M. Naumenko, and A. I. Zvyanin, Preprint FTINT, Khar'kov, May 1973.
[3]V. G. Bar'yakhtar, V. P. Prasnov, and V. L. Sobolev, Fiz. Tverd. Tela **15**, 3039 (1973) [Sov. Phys.-Solid State **15**, 2025 (1974)].
[4]M. P. Kashchenko, N. F. Balakhonov, and L. V. Kurbatov, Zh. Eksp. Teor. Fiz. **64**, 391 (1973) [Sov. Phys.-JETP **37**, 201 (1973)].
[5]B. Westwanski, JINR, E4-7625, Dubna, 1973.
[6]L. A. Shelepin, Zh. Eksp. Teor. Fiz. **54**, 1463 (1968) [Sov. Phys.-JETP **27**, 784 (1968)].
[7]R. O. Zaĭtsev, Preprint IAE-2361, Moscow, 1964.
[8]N. G. Chebotarev, Teoriya grupp Li (Theory of Lie Groups), Gostekhizdat, Moscow-Leningrad, 1940.
[9]L. S. Pontryagin, Nepreryvnye gruppy (Continuous Groups), Nauka, 1973, Chap. 11.
[10]V. G. Vaks, A. I. Larkin, and S. A. Pikin, Zh. Eksp. Teor. Fiz. **53**, 281, 1089 (1967) [Sov. Phys.-JETP **26**, 188, 647 (1968)].
[11]R. O. Zaitsev, Preprint IAE-2378, Moscow, 1974.

Translated by J. G. Adashko
26